THE EFFECT OF DIFFERENT ARRAY-CONFIGURATIONS ON THE ACCURACY OF PASSIVE ACOUSTIC LOCATION OF CETACEANS

J. Vallarta School of Engineering and Physical Sciences, Heriot-Watt University, Edinburgh, UK
R. McHugh
P. Record

1 INTRODUCTION

Hydroacoustic researchers use a number of passive acoustic techniques to determine cetacean localisation [1,2,3,4] at sea. These localisation techniques use a variety of hydrophone array-configurations. However, the array-configuration has a direct effect on location accuracy and must be considered carefully before deployment [5,6]. The following attributes of the array need to be considered: *number of receivers*; *array-geometry* and *overall aperture.* We compare ranges computed from three hydrophone array-configurations by a MATLAB based array-simulator.

2 METHOD AND MATERIALS

2.1 Hyperbolic Localisation

This paper is based on the use of the hyperbolic localisation technique [7] with an assumption of constant sound speed. This technique relies on the measurement of the time difference of arrival (TDOA) between two separate hydrophones as a sound wave arrives from a point source located in 3D space. The location of the source can be assumed to lie on a geometric hyperboloid surface. For multi-element arrays each pair of hydrophone elements will generate a hyperboloid surface and at the intersection of these surfaces the source will be located.

2.2 Simulator

Performing experiments at sea in order to evaluate array performance even for a small array of hydrophone elements is a complex and costly business. In order to assess the localisation performance of typical hydrophone array-configurations a full 3D simulation environment was developed using MATLAB Version 7.0 (Mathworks, Inc). The user is able to set the receiver position in the Cartesian plane (x, y, z) for between 2 and 6 elements in size via a graphical user interface. Straight line geometry is then used to compute the TDOA parameters from a known source location by assuming a constant sound speed. These parameters are entered into the simulator to compute a location. The difference between the known location and its computed location is then used as a metric to compare different array-configurations.

2.2.1 Simulation Settings

The minimum distance separation $\boldsymbol{L}$ of any two elements has been set to 7.5m. This distance represents the half a wavelength [8] for the minimum frequency of vocalisation of a sperm whale, 100Hz [9]. The notation used in this paper is that a *long aperture-array* is defined as an array having a distance separation equivalent to 8L. A *short aperture-array* is defined as have length of 2L.

The Simulator was exercised by twenty selected source vocalising positions $\boldsymbol{S_V}$ (S_{Vx}, S_{Vy}, S_{Vz}) around the receiver array. To achieve this, the origin receiver $\boldsymbol{r_1}$ (0, 0, r_{1z}) is chosen as the reference point. Then, for the horizontal-source range an imaginary circle of radius R_h *(L)* and origin r_1 is

created and used as the input variable on the simulator. The simulator computes all the S_V locations and repeats the same cycle for different R_h values, keeping always the same S_{Vz} depth-position (Fig. 1). For depth-source ranges, the same procedure is repeated for different S_{Vz} depth-positions, keeping always the same R_h value so that all scenarios are covered for the chosen array-configuration.

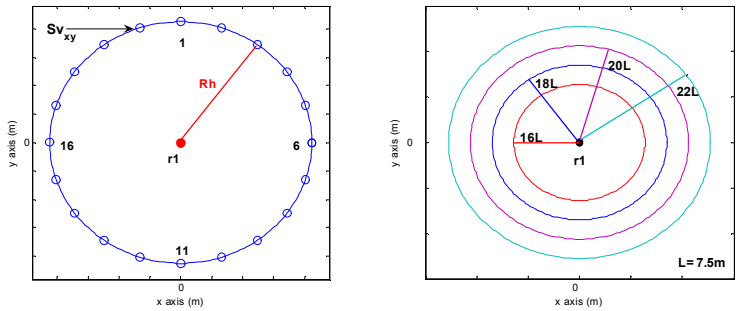

Figure 1. Scenario of twenty selected S_V locations lying on a circle of radius R_h and origin r_1

2.2.2 Localisation Error

The localisation error x_i is defined as the absolute difference between the known S_V position and the computed source location using the hyperbolic geometric algorithm. A primary localisation error results from the imprecision of the intersections of the hyperboloid surfaces for different S_V locations. Graphs of the *mean and variance localisation error* show the accuracy at each axis (x, y, z) for a given source range. Formally, the unbiased estimator of the mean and variance are represented by the equations (1) and (2) respectively.

$$\bar{x} = \frac{1}{n}\sum_{i=1}^{n}(x_i) \qquad (1)$$

$$\sigma^2 = \frac{1}{n-1}\sum_{i=1}^{n}\left(x_i - \bar{x}\right)^2 \qquad (2)$$

For each source range chosen there is a population of twenty different S_V positions around the receiver-array. When n=20 is the number of locations computed from sweeping the radii described in the last section. x_i is the calculated S_V location error and x bar and σ^2 are the mean and variance of such error. The square root of variance is of course standard deviation, and by invoking the central limit theorem it could be argued that it gives a measured of error of location although the computational errors from the hyperbolic solution are almost certainly not normal. The metric used for array comparison is set to be the average size of Sperm whale of about 15m [10] i.e. $\pm$7.5m.

3 RESULTS

3.1 Array-Configurations

The intersection of the hyperboloid surfaces determines the 3D source location [11]. Four receivers are sufficient to give an unambiguous range and bearing. With such information it is also possible to determine depth information. Four receivers offer a variety of different geometries [12]. For this exercise all the elements lie in the same horizontal plane, at a depth of 2L.

Three array-configurations are considered shown below in Figure 2. One of the simplest array-configurations with *four* receivers is the *square* geometry. Among its main features are two pairs of receivers {(r_1, r_2), (r_1, r_3)} with the same distance separation ***L*** and one pair (r_1, r_4) with different

dimensions as it is shown in Figure 1a. The *Y-shape* array-configuration with *four* receivers is arranged so that each arm {(r_1, r_2), (r_1, r_3), (r_1, r_4)} is the same length (Fig. 2b). The third array-configuration with *five* receivers has a *circular* geometry (Fig. 2c) such that each pair {(r_1, r_2), (r_1, r_3)} & {(r_1, r_4), (r_1, r_5)} has the same length.

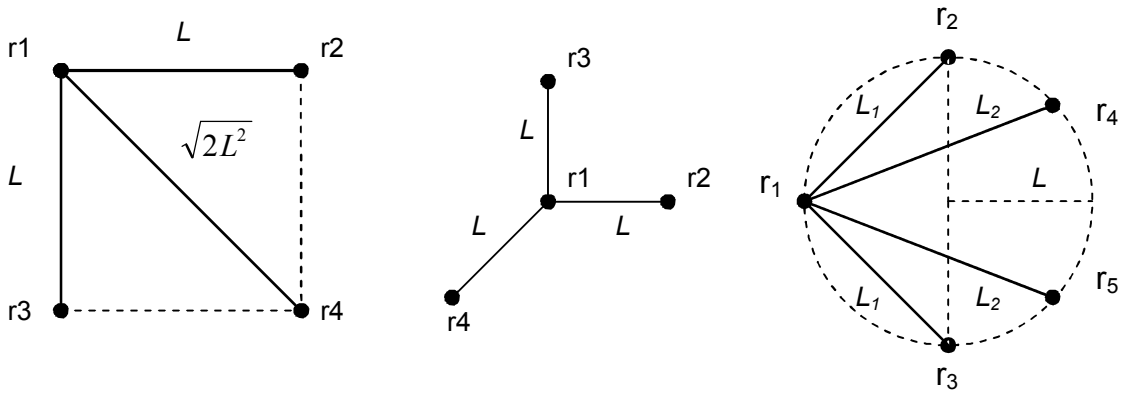

Figure 2. Array-Configurations, from left to right: Square, Y-shape, Circular

Each of these array-configurations was simulated to analyze the accuracy of both a short and a long aperture-array. The S_V position is varied in both planes, the horizontal (x-y axes) and the vertical (z-axis) as indicated above. The simulation specifications are shown in Tables 1-3 and the results in the following consecutive figures. The localisation error on each axis is highlighted. The plots in Figures 3, 5, and 7 show the *mean and variance localisation error* versus *horizontal-source range*. The plots in Figures 4, 6, and 8 show the *mean and variance localisation error* versus *depth-source range*. The horizontal lines at 7.5m define the maximum allowable tolerance, i.e. errors =< 7.5m are considered accurate.

3.1.1 Square-Array (4-elements)

Table 1 shows a matrix of apertures and source ranges in units of L. Four simulations were set to analyse the array localisation accuracy for both a short (2L) and a long (8L) aperture-array. Figure 3 shows that the short aperture-array can give accurate locations of S_V position up to the equivalent horizontal-source range of 20L (150m). After this point the array-configuration becomes inaccurate with a higher variance. On the other hand the long aperture-array reaches its accuracy limit at the equivalent horizontal range of 40L (300m) with respect the receiver origin. The use of a long aperture-array represents an accuracy improvement of double the distance. Figure 4 shows that the short-aperture array is accurate for short depth ranges of 16L (120m) then it exceeds the tolerance limit. With a long-aperture array, the accuracy of depth-source range improves to 22L (165m). A major cause of the inaccuracy of this configuration is due to the ambiguity caused by the end fire and broadside source-receiver positions. Also as the source goes deeper the curvature of the hyperboloid surface is reduced to almost a flat surface. Hence the depth error is always greater than the horizontal error. The asymmetry in localisation error between X and Y axes occurred as a function of the horizontal intersection of the hyperboloids for the twenty S_V positions varied in both planes.

Square-Array	**1a**	**1b**	**1c**	**1d**
Aperture-array	Short	Long	Short	Long
Horizontal-Source Range	**16L-24L**	**16L-42L**	20L	20L
Depth-Source Range	8L	8L	**8L-24L**	**8L-24L**

Table 1. Specifications for the group of Simulations No.1

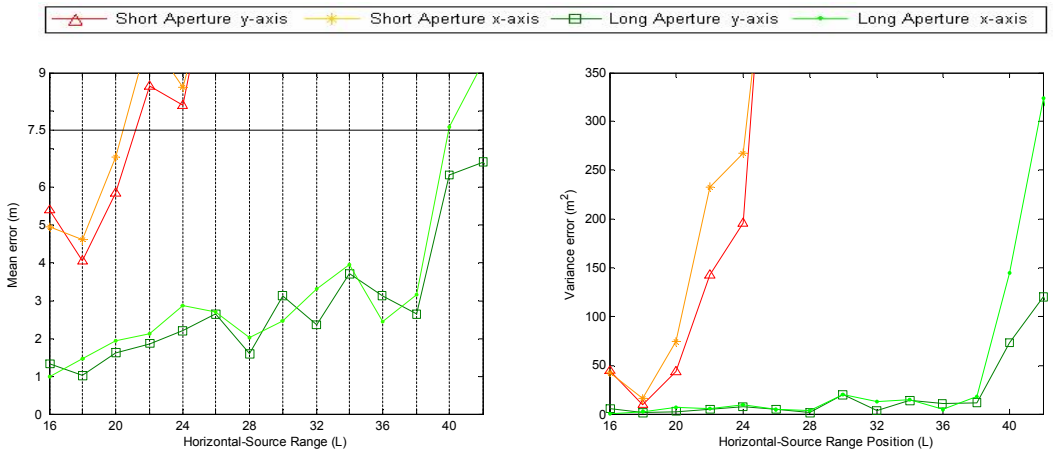

Figure 3. Mean (a) and Variance (b) horizontal error of a *Square-Array* (simulations 1a & 1b)

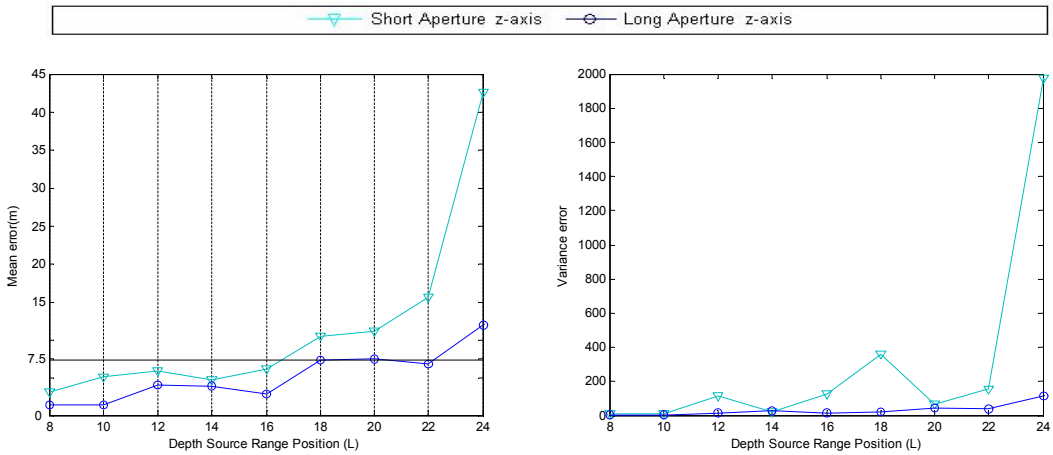

Figure 4. Mean (a) and Variance (b) depth error of a *Square-Array* (simulations 1c & 1d)

3.1.2 Y-shape-Array (4-elements)

This particular array-configuration is seen to be more accurate than the square for larger horizontal and depth ranges. Also the element-pair ambiguities are reduced compared to the square-array. Hence there is a noticeable improvement in accuracy in terms of the horizontal capabilities shown in Figure 5. The short-aperture array reaches the accuracy limit at the equivalent range of 34L (255m) and keeps a low variance error. The long aperture-array keeps below the tolerance limit up to the equivalent range of 56L (420m). The depth capabilities are shown in Figure 6. The short-aperture is able to give accurate locations within a depth range of 8-38L (60 to 285m). On the other hand the use of a long-aperture array allows us to have accurate readings for up to 40L (300m). This also represents a significant improvement in depth accuracy when compared to the square-array which reaches only one half of this depth. The hyperboloid intersection in the z-axis becomes inaccurate at greater depths.

Y-shape-Array	**2a**	**2b**	**2c**	**2d**
Aperture-array	Short	Long	Short	Long
Horizontal-Source Range	**16L-36L**	**16L-58L**	20L	20L
Depth-Source Range	8L	8L	**8L-42L**	**8L-42L**

Table 2. Specifications for Simulation No.2

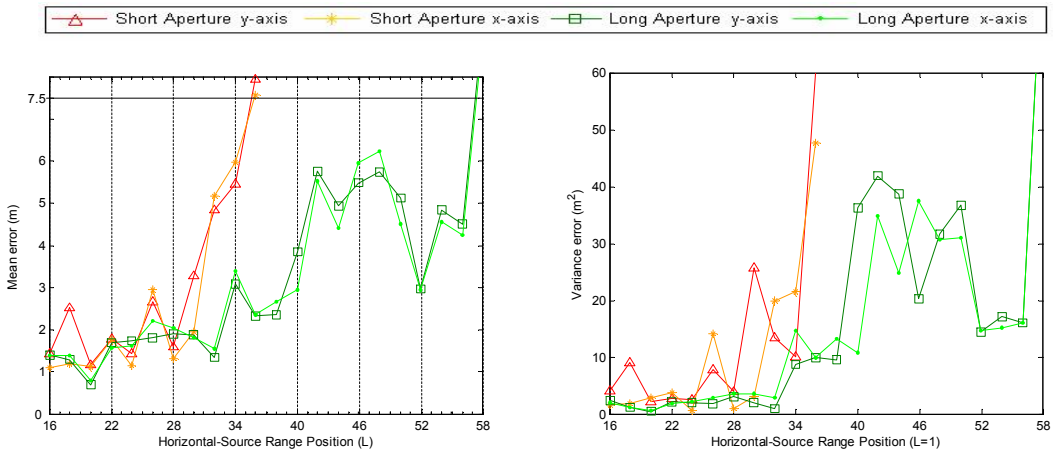

Figure 5. Mean (a) and Variance (b) horizontal error of a *Y-shape-Array* (simulations 2a & 2b)

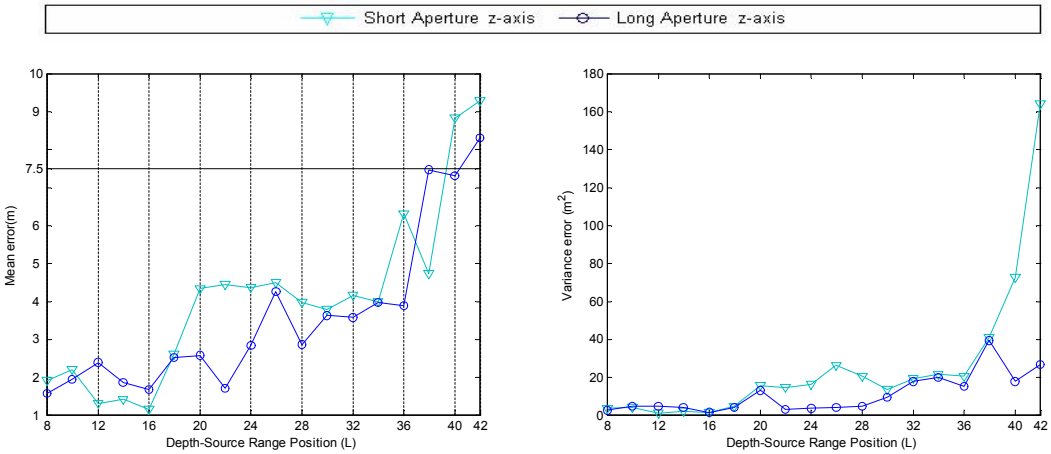

Figure 6. Mean (a) and Variance (b) depth error of a *Y-shape-Array* (simulations 2c & 2d)

3.1.3 Circular-Array (5-elements)

Of the three array-configurations, this is the most accurate for the twenty different source positions chosen. Figure 7 shows the improvement achieved through the use of an extra receiver to create a circular geometry. The accurate horizontal range reached for the short aperture-array is 90L (675m). The long aperture-array generates noticeable improvements on the localisation accuracy. It is able to reach a horizontal range of 254L (1.9km). The variance error is the lowest of the three array-configurations showed. Finally in the category of depth range in Figure 8, the short-aperture proves to be accurate for only depths of up to 26L (195m). The long-aperture is only accurate for depths up to 34L (255m).

Circular-Array	3a	3b	3c	3d
Aperture-array	Short	Long	Short	Long
Horizontal-Source Range	**16L-92L**	**16L-272L**	20L	20L
Depth-Source Range	8L	8L	**8L-38L**	**8L-38L**

Table 3. Specifications for Simulation No.3

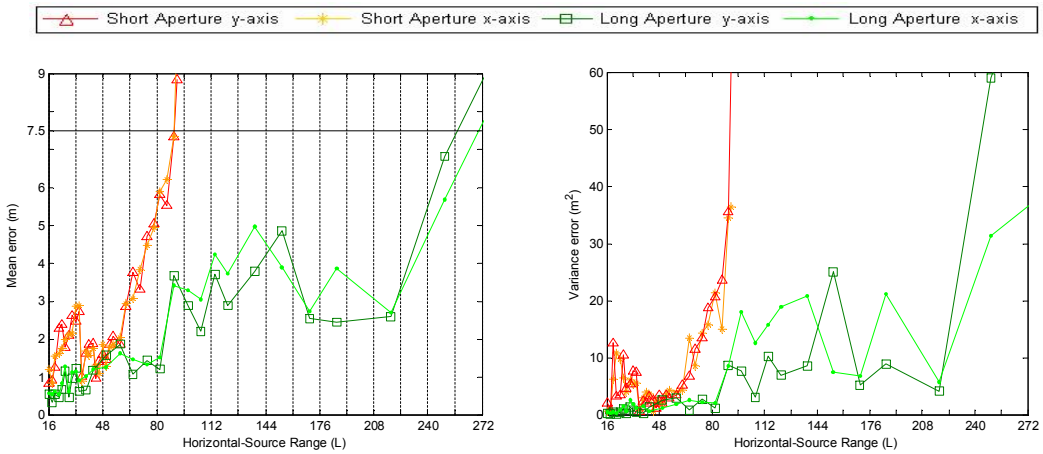

Figure 7. Mean (a) and Variance (b) horizontal error of a Circular-Array (simulations 3a & 3b)

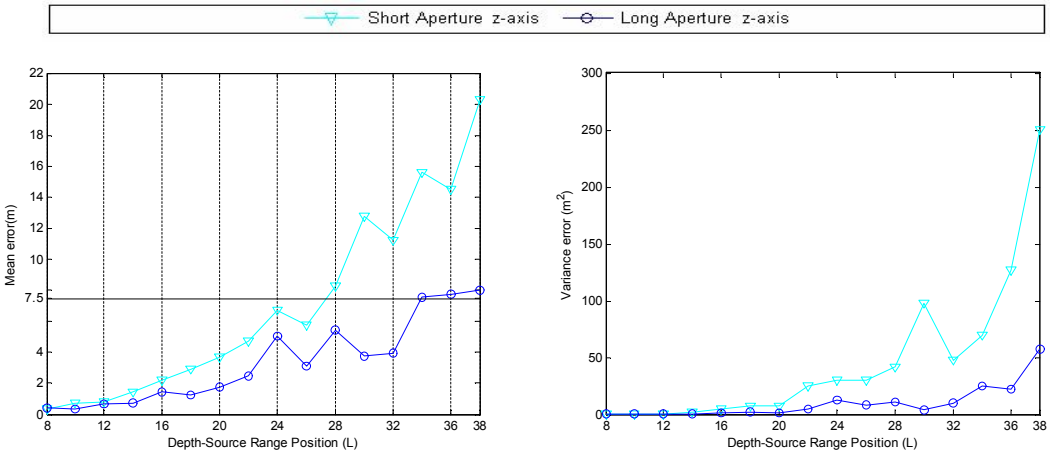

Figure 8. Mean (a) and Variance (b) depth error of a Circular-Array (simulations 3c & 3d)

3.2 Array Comparison

Table 4 and Figures 9 and 10 summarize the maximum horizontal-range and depth-range of the three array-configurations using a short and a long aperture-array.

From the three array-configurations investigated, the circular-array proves to give the largest horizontal range for both short and long aperture-arrays. For short apertures the circular-array has 4.5 times more horizontal range than the square-array and 2.6 times more than the Y-shape-array. For long apertures the circular-array has 6 times more horizontal range than the square-array and 4.5 times more than the Y-shape-array. However, the Y-shape-array has better depth range than the circular-array (Table 4).

Source Location	Aperture	Square		Y-shape		Circular	
		x	y	x	y	x	y
Horizontal Range	2L	20L	20L	34L	34L	90L	90L
	8L	40L	42L	56L	56L	272L	254L
Depth Range	2L	16L		38L		26L	
	8L	22L		40L		34L	

Table 4. Summary of the maximum ranges reached for each array-configuration

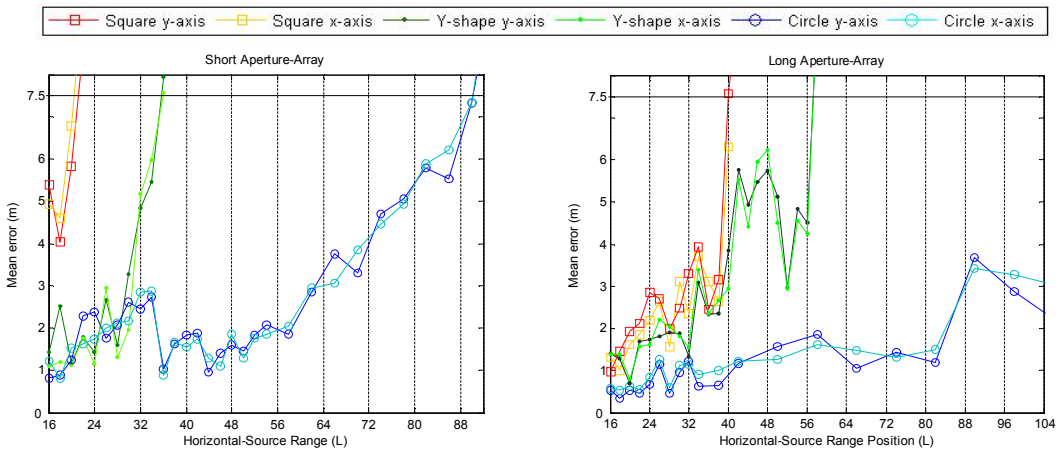

Figure 9. Comparison of the three Array-Configurations on a horizontal-source range

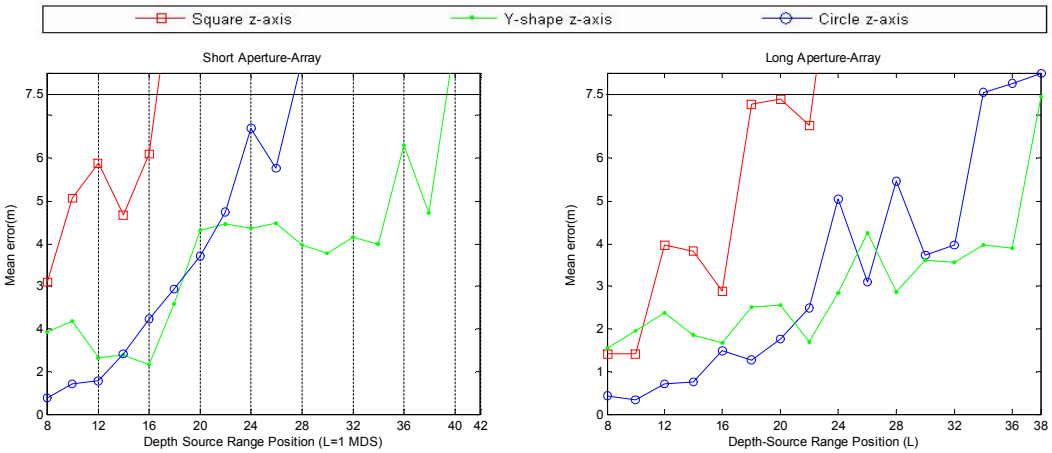

Figure 10. Comparison of the three Array-Configurations on a depth-source range

In both short and long apertures the Y-array gives the deepest range. For short apertures the y-shape-array has 2.4 times more depth range than the square-array and 1.5 times more than the circular-array. For long apertures the Y-shape-array has 1.8 times more depth range than the square-array and 1.2 times more than the circular-array. It is also from both categories (horizontal-range and depth-range) the array-configuration with less range variation when the aperture-array changes. Finally, the square array produces the shortest horizontal and depth range for a short or long aperture-array.

4 DISCUSSION AND CONCLUSIONS

Although theoretically more receivers will improve the localisation accuracy, the other most important factor is the array-geometry. For instance, the four receivers distributed in Y-shape-array gave better ranges than the four receivers in the square-array for both long and short aperture-arrays. Furthermore, when an extra receiver was added to create a circular-array, the horizontal-source localisation had a noticeable improvement.

The clearest result these simulations have is range improves with longer apertures. For instance, the square-array improved twice its range; the Y-shape 1.65 times; and the circular 2.82 times; an average ratio of more than the double. However if we measure the ratio of *range to size of aperture* for each array-configuration; we found that such a ratio decreases for longer apertures due to the hyperbolic localisation error caused by the small angle between the hyperbolic surfaces. Therefore,

lengthening the aperture-array may be one solution to enable location of a more distant source. However, this implies a more complicated deployment with inaccurate locations when the source is at broadside to a pair of array elements.

In terms of depth the Y-shape-array is preferred, however, its operational depth ranges (285-300m) are still relatively short compared to typical Sperm whale depth profiles of 800m average [13,14]. The lack of depth-source location accuracy is due mainly to the nature of the hyperboloid geometric surface. However, we found that increasing the aperture-array length would aid in depth location.

So in summary, a square-array is not a recommendable configuration for deployment. A Y-shape-array represents a simple geometry that provides accurate source locations for long and deep ranges. A circular-array appears to offer greater range capability without the need to have an excessive aperture.

REFERENCES

1. D.H. Cato. 'Simple methods of estimating source levels and locations of marine mammals sounds', Journal of the Acoustic Society of America 104(3): 1667-1678 (1998).
2. D.S. Clark, J. Flattery, R. Gisiner, J. Schilling, T. Sledzinski, and R. Trueblood. 'MMATS: Acoustic localization of whales in real time over large areas', Journal of the Acoustic Society of America 96: 3250 (1994).
3. W.A. Watkins, and W.E. Schevill. 'Sound source location by arrival-times on a non-rigid three-dimensional hydrophone array', Deep-Sea Research 19: 691-706 (1972).
4. W.C. Cummings, and D.V. Holliday. 'Passive acoustic location of bowhead whales in a population census off Point Barrow, Alaska', Journal of the Acoustic Society of America 78, 1163–1169 (1985).
5. T-J., Shiao, and J.R. Buck. 'Optimal array design and sensitivity for mode filtering'. Journal of the Acoustic Society of America 109(5): 2496 (2001).
6. A.H. Nuttall, and B.A. Crag. 'Approximations to Directivity for Linear, Planar, and Volumetric Apertures and Arrays', IEEE Journal of Oceanic Engineering 6(3): 383-398 (2001).
7. J. L. Spiesberger, and K. M. Fristrup. 'Passive Localization of Calling Animals and Sensing of their Acoustic Environment Using Acoustic Tomography'. The American Naturalist 135: 107-153 (1990).
8. L. Rayleigh, 'On the Perception of the Direction of Sound', Proceedings of the Royal Society A, vol. 83, pp.61-64 (1909)
9. P.T. Madsen, R .Payne, N.U. Kristiansen, M. Wahlberg, I. Kerr and B. Mohl. 'Sperm whale sound production studied with ultrasound time/depth-recording tags'. The Journal of Experimental Biology 205, 1899–1906 (2002).
10. H. Whitehead. Sperm Whales: Social Evolution in the Ocean. *The University of Chicago Press*, (2003).
11. M. Wahlberg. 'Comparing a linear with a non-linear method for acoustic localization', Proceedings of the 2003 Workshop on Detection and Localisation of Marine Mammals using Passive Acoustics, Journal of the Canadian Acoustics 32(2), (2004).
12. J.L. Spiesberger. 'Hyperbolic location errors due to insufficient numbers of receivers', Journal of the Acoustic Society of America 109(6): 3076-3079 (2001).
13. M. Amano, and M. Yoshioka. 'Sperm whale diving behaviour monitored using a suction-cup-attached TDR tag', Marine Ecology Progress Series 258: 291-295 (2003).
14. P.J.O. Miller, M.P Johnson, P.L Tyack, and E.A. Terray. 'Swimming gaits, passive drag and buoyancy of dividing sperm whales *Physeter macrocephalus*', The Journal of Experimental Biology 207: 1953-1967 (2004).